Two Dimensional Phase Separation for Co Adsorbed on Si(111)

R. J. Phaneuf
Department of Physics, University of Maryland-College Park, College Park, Maryland 20742-4111

Y. Hong, S. Horch, and P. A. Bennett
Department of Physics and Astronomy, Arizona State University, Tempe, Arizona 85287

(Received 15 August 1996)

We have used low energy electron microscopy to monitor the high-temperature behavior of surface phases in the Co/Si(111) system at submonolayer coverages. We observe a reversible phase separation from a disordered "(1×1)" phase to well-defined coexisting regions of ordered (7×7)-reconstructed and disordered phases. The transition temperature is depressed by nearly 200 °C by the addition of 0.1 monolayer of cobalt. The shape of the coverage-temperature phase boundary allows us to estimate the latent heat of the (7×7) order-disorder transition. [S0031-9007(97)03320-6]

PACS numbers: 68.35.Rh, 61.16.–d, 81.30.Hd, 82.65.Dp

Surface effects in bulk alloying systems is a topic of long-standing interest, with important fundamental and practical aspects such as surface segregation, grain boundary embrittlement, impurity gettering, and faceting behavior. More recently, studies of heteroepitaxial growth have highlighted the importance of understanding the thermodynamics of coupling between overlayers and substrate. In view of the above, and the ubiquity of compositional phase separations in bulk systems, it is perhaps surprising to find no report in the literature of two-dimensional (2D) phase separation of a surface segregant. One reason for this is that surface segregants in most systems are essentially equilibrated with the bulk at temperatures of interest. This results in a single-phase surface structure at all temperatures, even though the surface may exhibit a phase transition in which coverage increases suddenly below a critical temperature, following a miscibility gap phase diagram [1]. A second reason may be that it is experimentally difficult to observe phase separation with diffraction techniques, which are almost exclusively used for such studies. On the other hand, phase separation is directly observable using surface imaging techniques such as low energy electron microscopy (LEEM), which is capable of distinguishing phases with differing atomic structure, with approximately 100 Å lateral resolution, high contrast, and at high temperature [2]. In this paper, we report direct LEEM observations of a reversible phase separation between ordered and disordered 2D phases for a prototype metal-semiconductor system, Co/Si(111).

Previously, Bennett *et al.*, using scanning tunneling microscopy (STM) and medium energy ion scattering (MEIS) found that a remarkably stable "ring-cluster" (RC) structure exists for all group VIII metals adsorbed on Si(111), with each RC consisting of a single metal atom in a substitutional silicon site plus an overlying ring of six silicon adatoms [3]. In the case of cobalt an ordered arrangement of RC's with a $(\sqrt{7} \times \sqrt{7})R19.1°$ unit cell forms at the close-packed density of $\frac{1}{7}$ ML. At lower coverages a disordered, or "(1×1)," variable density lattice gas arrangement of RC's exists at domain boundaries of the (7×7) reconstruction. It was not clear from STM "quench and look" observations whether these structures exist at high temperature or what their interactions might be.

As we describe below, we find that, at high temperatures, RC phases of Co/Si(111) are stable against the dissolution of Co into bulk silicon or condensation into bulk silicides on an observable time scale. With increasing Co coverage we observe a sequence of single and coexisting ordered and disordered surface structures suggestive of binary eutectic behavior. We analyze the shape of the boundary separating a uniform disordered RC-containing phase from coexisting ordered (7×7) and disordered (1×1)-RC phases, using a local equilibrium-based description, based on the reversability of transitions across it.

The principle of operation of the LEEM is described in detail elsewhere [2], as is the microscope used in this work [4]. The base pressure in the instrument was 2×10^{-10} torr. The Si sample was heated via electron bombardment. Temperature measurement was via an infrared pyrometer which was calibrated at the clean surface (7×7) to (1×1) transition temperature [5]. Sample cleaning was done by heating briefly in UHV to 1250 °C. Evaporative deposition was done by direct current heating of a high purity Co wire, and measured *in situ* using a quartz crystal thickness monitor, calibrated from the known $\frac{1}{7}$ ML (1 ML $= 7.8 \times 10^{14}$ atom/cm^2) saturation coverage of the $(\sqrt{7} \times \sqrt{7})R19.1°$ phase [3].

We first explored the phase diagram of Co/Si(111) by slowly increasing the amount of Co on the surface at a fixed temperature. The LEEM images of Fig. 1 show a Si(111) surface just before and during deposition of Co at a flux of 0.0017 ML/s and a temperature of 735 °C. Figure 1(a) shows the surface shortly after cleaning, and before deposition starts, on which we observe a (7×7) low-energy electron diffraction (LEED) pattern. This image is nearly featureless except for a step- "pinning center," which provides a fixed reference point in the

image. Panels (b)–(f) show the time evolution of this surface as Co is deposited. Already, by 0.02 ML, the formation of a second (dark) structure is evident. In LEEM, the images give a spatial map of the electron reflectivity, and the contrast observed in these bright-field LEEM images is consistent with measurements of different LEED IV profiles for the specular reflection above and below the (7×7) to (1×1) transition [5]. As the Co coverage is increased, the dark regions in the image form at, and spread outward from, atomic height steps and domain boundaries of the (7×7) reconstruction at the expense of the existing (7×7) regions, indicating a phase separation. The dark regions are evidently the same (1×1)-RC structure seen in STM images at room temperature [3]. By a coverage of 0.1 ML [panel (d)] the dark regions essentially cover the entire surface. The LEED pattern from this surface shows only (1×1) reflections plus a diffuse background. The growth mode of the (1×1)-RC structure indicates limited solubility of RC's in regions of the ordered (7×7) phase. We have earlier observed a qualitatively similar separation for Ni/Si(111) [4].

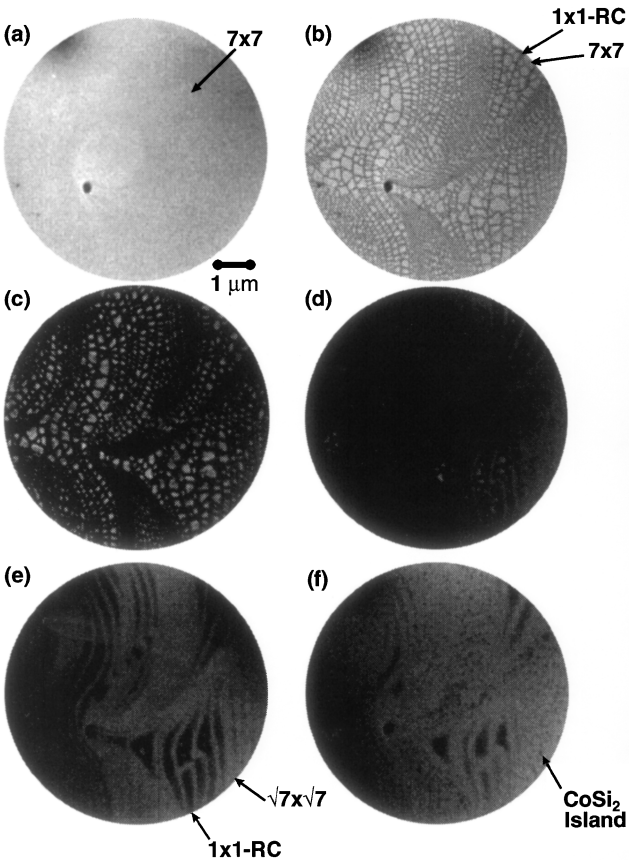

FIG. 1. Bright field LEEM images of Si(111) surface during deposition of Co at 735 °C at coverages of (a) 0.00 ML, (b) 0.02 ML, (c) 0.04 ML, (d) 0.10 ML, (e) 0.13 ML, and (f) 0.16 ML. The (7×7) appears as white, the (1×1) RC as black, and the $(\sqrt{7} \times \sqrt{7})$ as gray at these conditions. Here and in Fig. 3 the incident energy is 3.6 eV, incident angle is 0°, and the field of view is 7 μm.

As the Co dose continues, a third structure, dark gray under these imaging conditions, becomes evident. It also grows inward from step edges. By $\frac{1}{7}$ ML [panel (e)] it nearly covers the surface. At this coverage the surface has a LEED pattern consisting of two orientational domains of $(\sqrt{7} \times \sqrt{7})R19.1°$ reflections. Beyond approximately $\frac{1}{7}$ ML, we begin to observe the formation of small particles which we believe to be $CoSi_2$ islands [6].

Interestingly, the observed sequence of surface phases formed during Co deposition follows that of a bulk binary eutectic system above the eutectic temperature [7]. In the top of Fig. 2 we show the average image intensity from a multidomain region on the surface, taken from the sequence of Fig. 1. At the bottom of the figure we show a schematic eutectic phase diagram for the case of negligible mutual solubility of RC's and patches of (7×7) in the (7×7) and $(\sqrt{7} \times \sqrt{7})$ ordered phases, respectively. Since the average image intensity is a linear combination of intensities from the coexisting phases, the continuous changes in gray scale are qualitatively consistent with moving along the constant temperature coexistence "tie lines" of this diagram. The contrast between (7×7), (1×1) RC, and $(\sqrt{7} \times \sqrt{7})$ varies with energy, and can even reverse. For these imaging conditions, with the intensity from the (1×1) RC being the lowest, the minimum in

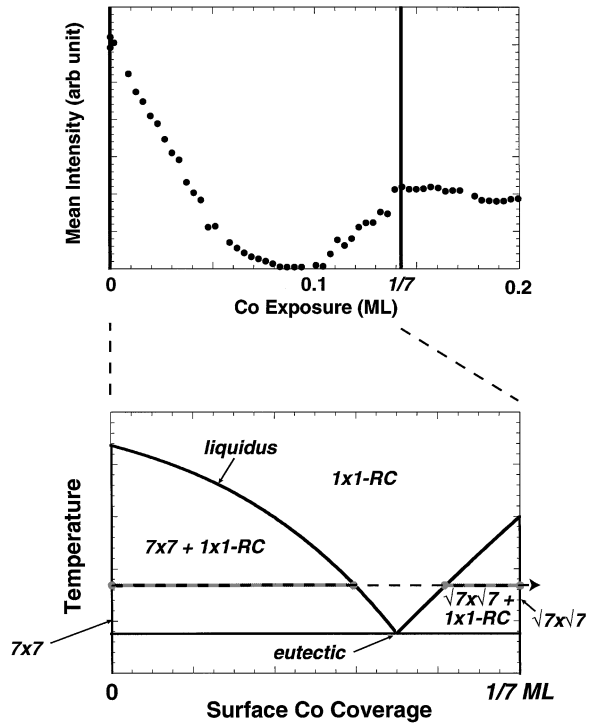

FIG. 2. Top: average image intensity during Co deposition as in Fig. 1 for a selected multidomain region of the images in which the terrace widths range over 600 ± 200 Å. Bottom: schematic equilibrium phase diagram for surface phases of Co on Si(111). Dashed arrow shows the trajectory for the Co deposition experiment of Fig. 1. Gray bars show tie lines connecting points of coexisting phases in two-phase regions. Note the horizontal scale change from the top panel.

the average intensity shown in the bottom of Fig. 2 gives the approximate median coverage for a single- (1×1)-RC phase, and an approximate location of the eutectic composition.

To check for reversibility across the phase boundary separating disordered (1×1) RC from coexisting ordered (7×7) and disordered (1×1)-RC structures, we imaged the surface during heating and cooling experiments at a series of different Co coverages, as shown in Fig. 3 for a Co coverage of 0.04 ML. The (7×7)-reconstructed (light) regions are segregated at the step edges. As the temperature is increased, these regions shrink [panels (b) and (c)] and completely disappear at 826 °C, leaving a surface which is entirely (1×1) RC [panel (d)]. Lowering the temperature results in a reappearance of the (7×7) reconstruction at step edges at very nearly the same temperature, 824 °C. Further cooling results in a growth of the (7×7) outward from the step edges at the expense of the (1×1)-RC regions [panels (e) and (f)]. A slight difference in the arrangement of (7×7) regions in panels (a) and (f) comes from the nucleation of the (7×7) at step edges during cooling through the phase boundary, in contrast to the nucleation of the (1×1) RC at domain boundaries of the (7×7) during deposition of Co. Images acquired during subsequent heating and cooling cycles produced arrangements essentially identical to that of panel (f) at the same temperature. The measured transition temperatures vs Co coverage are plotted in Fig. 4. Above 800 °C the transition temperatures on heating and cooling are very nearly the same, provided that the total time at temperatures near 850 °C is less than a few minutes. Beneath 800 °C, a small hysteresis is observed. The phase separation from uniform (1×1) RC into coexisting (7×7) and (1×1) RC is otherwise reversible with temperature.

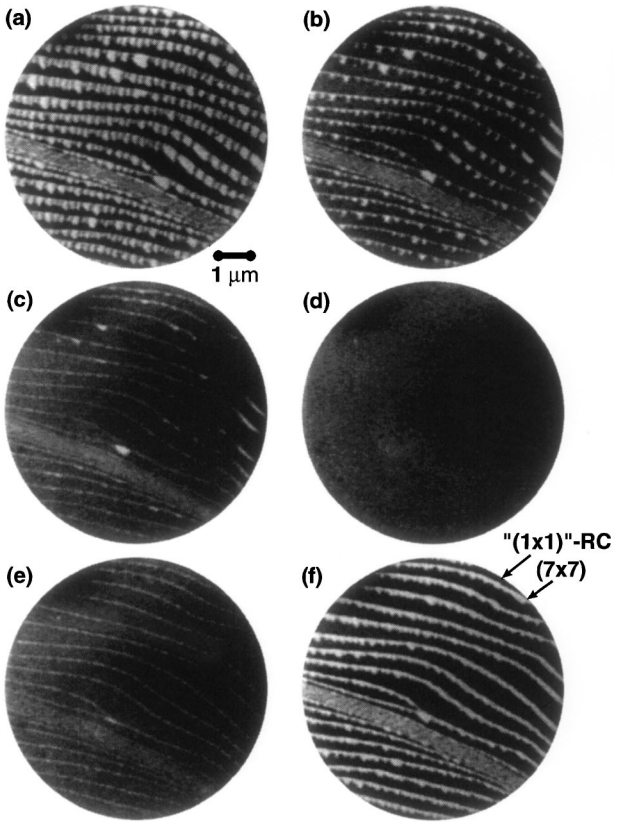

FIG. 3. Bright field LEEM images of Si(111) during heating and cooling sequences after deposition of 0.04 ML Co at 767 °C. (a) $T = 768$ °C (first heating). (b) $T = 806$ °C (heating). (c) $T = 816$ °C (heating). (d) $T = 827$ °C (begin cooling). (e) $T = 816$ °C (cooling). (f) $T = 768$ °C (cooling).

Attempts to observe reversible transitions across other phase boundaries show that a eutectic-based model can provide only partial understanding of the early stages of the growth of Co on Si(111). Transitions across the boundary separating the $(\sqrt{7} \times \sqrt{7})$ and (1×1)-RC structures are not reversible due to the formation of silicide islands at coverages near $\frac{1}{7}$ ML, which locally deplete the surface of Co. We also find that the separation between (7×7) and (1×1) becomes increasingly sluggish for temperatures below that for the growth sequence of Fig. 1, precluding observation of transitions across the lower boundary, to coexisting (7×7) and $(\sqrt{7} \times \sqrt{7})$ structures, on the time scale of our observations. However, as we observe that transitions across (7×7) to (1×1)-RC phase boundary are reversible, we next consider a thermodynamic model to explain its shape.

The clean-surface Si(111)-(7×7) to (1×1) order-disorder transition is believed to be first order [8] so that a latent heat, which is proportional to the difference in entropy between the two phases at the transition temperature, must be added to disorder the (7×7). In spite of great interest in the (7×7) to (1×1) transition [5,8], there have been very few published values for this fundamental thermodynamic parameter [9]. Next we show that the shape of the transition temperature vs Co coverage curve shown in Fig. 3 allows us to estimate the clean surface-transition latent heat.

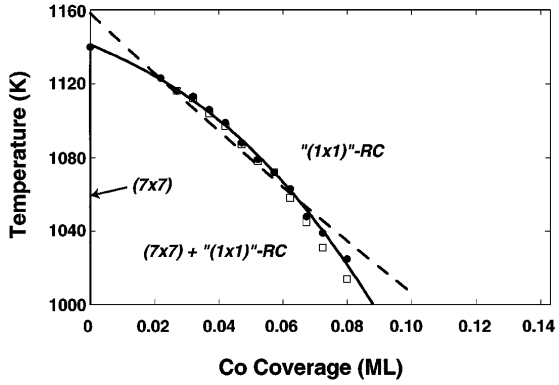

FIG. 4. Temperature at which (7×7)-reconstructed (white) regions completely disappear from LEEM image on heating (solid circles) and reappear on cooling (open squares) vs ring-cluster coverage (Θ_{Co}) for Co/Si(111). The dashed curve shows the optimum fit to the form of Eq. (1). The solid curve shows the optimum fit of the transition temperature on heating (solid circles) to the form of Eq. (2).

The depression of the (7×7)-disordering temperature can be understood qualitatively as coming from the energy cost of having RC's within regions of (7×7) reconstruction rather than within the disordered phase. The simplest model for this system is a noninteracting lattice gas of RC's. Equating the 2D spreading pressures [10] in the (7×7) and (1×1)-RC phases and assuming negligible solubility of RC's in the (7×7) ordered phase yields

$$\ln(1 - \Theta_{\mathrm{RC}}) = h^{7\times7\text{-}1\times1}\alpha/k_B(1/T_0 - 1/T), \quad (1)$$

where Θ_{RC} is the RC coverage (which is equal to the Co coverage), $h^{7\times7\text{-}1\times1}$ is the latent heat of the (7×7) to (1×1) transition, α is the area of a (1×1) unit cell, and T_0 is the disordering temperature for the clean Si(111) surface. The best fit of our data to the form of Eq. (1) is shown by the dashed curve in Fig. 4. The fitted curve is nearly linear, with slightly upward curvature, and deviates systematically from the experimental data, which displays the opposite curvature. A natural refinement of the model is to include an "excess enthalpy," h^{XS}, due to interactions between RC's. We do not know the functional form of this interaction *a priori* [11], but consider dipole-dipole interactions, either strain mediated [12] or electrostatically mediated, to be plausible. Such interactions fall off as the inverse cube of the separation, and as the average separation is proportional to the square root of the coverage; this leads to a factor of $\Theta_{\mathrm{RC}}^{3/2}$ per dipole in the interaction term. Multiplying by the density of dipoles gives another factor of Θ_{RC} for an overall $\Theta_{\mathrm{RC}}^{5/2}$ dependence for h^{XS} and a spreading pressure equation as follows:

$$\ln(1 - \Theta_{\mathrm{RC}}) = h^{7\times7\text{-}1\times1}\alpha/k_B(1/T_0 - 1/T) - c\Theta_{\mathrm{RC}}^{5/2}\alpha/k_BT\,. \quad (2)$$

The resulting fit is shown by the solid curve in Fig. 4. The agreement between the measured heating curve and a fit to this form is excellent [11].

The best fit of our measured disordering temperatures to the form giving by Eq. (2) yields a latent heat of 146 ± 64 meV/(1×1)–unit cell for the (7×7) to (1×1) transition. This is approximately $1.5k_BT_0$, and thus reasonable based upon the clean surface transition temperature. It is of the same order of magnitude as that estimated by Williams *et. al.* [9] from a completely different method.

Finally, we considered the atomistic meaning of the excess enthalpy, h^{XS}. The fit to a $\Theta_{\mathrm{RC}}^{5/2}$ dependence yields h^{XS} equal to 4.4 ± 2.0 eV Å^5 $\Theta_{\mathrm{RC}}^{5/2}/(1 \times 1)$-cell, with the sign indicating a repulsion between RC's. Of course, the interaction must become slightly attractive near the $\sqrt{7}$-spacing, otherwise the ordered phase would not form. (At high temperatures, entropy favors the (1×1)-RC phase, however, and thus the $(\sqrt{7} \times \sqrt{7})$ does not begin to form until the coverage approaches $\frac{1}{7}$ ML.) To extract a value of the pairwise interaction from our data, we evaluate h^{XS} at an average separation of twice the $\sqrt{7}$ spacing, corresponding to a coverage of 0.036 ML, which is near the middle of the range of the fit of Fig. 4. At this coverage the interactions between ring clusters raise the energy of the surface by 1.1 ± 0.5 meV/(1×1)–unit cell, or 30 ± 14 meV/RC. Equating this value to the sum of the interactions of an individual RC with all of its neighbors, we estimate a repulsive interaction potential between individual pairs of RC's of 39 ± 18 eV Å$^3/r^3$.

In summary, we find that the observed phase separation between ordered and disordered surface phases of Co adsorbed on Si(111) is in good agreement with a local-equilibrium thermodynamic model of a solution with small mutual solubilities in the ordered phases. This model allows us to estimate the latent heat of disordering of the (7×7) reconstruction and the interaction between Co-containing ring clusters on the surface. Finally, we note that it is the use of direct imaging in LEEM which makes possible the identification of the phase separation between ordered and disordered structures, and the precision of the LEEM determination of the separation temperature which allows the evaluation of RC-interaction enthalpy and the latent heat of the (7×7) to (1×1) transition.

We thank N. C. Bartelt for a number of fruitful conversations, and a careful reading of the manuscript. This work was supported by the NSF under Grant No. DMR9528503. One of us (R.J.P.) received support from the Laboratory for Physical Sciences and an NSF-MRG.

[1] P. Wynblatt, W.-C. Cheng, and Y. Liu, Prog. Surf. Sci. **48**, 261 (1995).
[2] E. Bauer and W. Telieps, Scanning Microsc. Suppl. **1**, 99 (1987).
[3] P. A. Bennett, M. Copel, D. Cahill, J. Falta, and R. M. Tromp, Phys. Rev. Lett. **69**, 1224 (1992); S. A. Parikh, M. Y. Lee, and P. A. Bennett, J. Vac. Sci. Technol. A **13**, 1589 (1995).
[4] P. A. Bennett, M. Y. Lee, S. A. Parikh, K. Wurm, and R. J. Phaneuf, J. Vac. Sci. Technol. A **13**, 1728 (1995).
[5] P. A. Bennett and M. B. Webb, Surf. Sci. **104**, 74 (1981).
[6] P. A. Bennett, S. A. Parikh, M. Y. Lee, and D. G. Cahill, Surf. Sci. **312**, 377 (1994).
[7] F. Daniels and R. A. Alberty, *Physical Chemistry* (Wiley, New York, 1975), 4th ed.
[8] W. Telieps and E. Bauer, Surf. Sci. **162**, 163 (1985).
[9] An entropy difference between (1×1) and (7×7) phases of $0.6k_B/(1 \times 1)$–unit cell is estimated in E. D. Williams, R. J. Phaneuf, J. Wei, N. C. Bartelt, and T. L. Einstein, Surf. Sci. **294**, 219 (1993), corresponding to a latent heat of 59 meV/(1×1)–unit cell.
[10] T. L. Hill, *An Introduction to Statistical Thermodynamics* (Addison-Wesley, Reading, MA, 1960).
[11] A Θ_{RC}^2 dependence gives a similarly good fit to our data as that shown in Fig. 4, and yields a latent heat of 218 meV/(1×1)–unit cell and an excess enthalpy of 2.4 eV Å^4 $\Theta_{\mathrm{RC}}^2/(1 \times 1)$–unit cell.
[12] J. M. Rickman and D. J. Srolovitz, Surf. Sci. **284**, 211 (1993).